ESLAB #53: The *Gaia* Universe
Edited by J.H.J. de Bruijne

# Periodic Variables as Distance Indicators in the *Gaia* era

Xiaodian Chen[1], Shu Wang[1,2], Richard de Grijs[3,4,5], Licai Deng[1,6]

[1] Key Laboratory for Optical Astronomy, National Astronomical Observatories, Chinese Academy of Sciences, 20A Datun Road, Chaoyang District, Beijing 100012, People's Republic of China
[2] Kavli Institute for Astronomy & Astrophysics, Peking University, Yi He Yuan Lu 5, Hai Dian District, Beijing 100871, People's Republic of China
[3] Department of Physics and Astronomy, Macquarie University, Balaclava Road, Sydney, NSW 2109, Australia
[4] Research Centre for Astronomy, Astrophysics and Astrophotonics, Macquarie University, Sydney, NSW 2109, Australia
[5] International Space Science Institute–Beijing, 1 Nanertiao, Zhongguancun, Hai Dian District, Beijing 100190, People's Republic of China
[6] Department of Astronomy, China West Normal University, Nanchong, People's Republic of China

## Abstract

Periodic variable stars, such as Cepheids, RR Lyrae, eclipsing binaries, and long-period variables, are important distance indicators. Historically, distances to some open clusters, globular clusters, Milky Way dwarf galaxies, and nearby galaxies are well determined based on these distance indicators. However, both the rapid development of large, wide-field instruments and new insights offered by infrared facilities have stimulated research of variable stars. The role of variables in the context of the distance scale should be updated. With the unprecedented *Gaia* second Data Release (DR2) parallaxes, the precision of the W UMa-type contact binary period–luminosity relation (PLR) is better than 6%. The significant number of the contact binaries makes them an important distance tracer. The known number of classical Cepheids in the Milky Way's disk has been increasing rapidly in recent years. Based on Cepheid distances, a new 3D map of the Milky Way's stellar disk has been constructed that is both intuitive and complete. In the outer disk, the stellar disk agrees with the gas disk in terms of their amplitudes. The outer disk is warped, and the morphology is complicated since the warp exhibits precession. In the next three years, new periodic variables will be detected. Based on a large sample of these variables, the distance and structure of our Milky Way, the Local Group, and nearby galaxies will be better understood.

## 1 Introduction

Periodic variables stars are stars exhibiting regular variations in their luminosity. Since their periods are directly or indirectly correlated to their luminosity, periodic variables usually follow period–luminosity relations (PLRs). Based on these tight PLRs, periodic variables play an important role in distance measurements.

In recent years, due to the development of new instruments and techniques, the number of periodic variables has increased rapidly. The Catalina survey found about 110,000 periodic variables in the northern and southern skies (Drake *et al.*, 2014, 2017). The *Wide-field Infrared Survey Explorer* (WISE) catalog of periodic variable stars found about 35,000 periodic variables (Chen *et al.*, 2018b), and 90% of them are located in the Galactic plane. This catalog also extends the scope of variables to the mid-infrared bands. The Asteroid Terrestrial-impact Last Alert System (Heinze *et al.*, 2018, ATLAS) found about 90,000 periodic variables down to $r \sim 18$ mag. The All-Sky Automated Survey for Supernovae (Jayasinghe *et al.*, 2018, ASAS-SN) found an additional $\sim 27{,}000$ periodic variables. The *Gaia* second Data Release (Gaia Collaboration *et al.*, 2018, DR2) also detected a large number of periodic variables (Clementini *et al.*, 2019; Mowlavi *et al.*, 2018), and many more improvements will be achieved in *Gaia*'s future data releases.

Given this huge increase in their number, periodic variables are more and more important in tracing the Milky Way's structure. Classical Cepheids, the young tracers (Matsunaga *et al.*, 2018), are suitable to trace the whole thin disk and the spiral arms. Due to the high luminosities and tight PLRs of Cepheids, they can be used to trace an intuitive 3D map of the disk at high accuracy (Chen *et al.*, 2019). W UMa-type (late-type) contact binaries (CBs) are intermediate-age distance tracers (Chen *et al.*, 2016). Since they represent a significantly large number of contact binaries, they are suitable to study the structure of the solar neighborhood and the Galactic bulge. Contact binaries can also be used to constrain the phase mixing in the disk (Antoja *et al.*, 2018). RR Lyrae are old distance tracers and usually used to study the halo, bulge, dwarf galaxies and substructure. In addition, Miras and type-II Cepheids (Bhardwaj *et al.*, 2017) provide distance information for some regions of the Milky Way.

In this paper, we present the PLRs of W UMa-type contact binaries that were determined using *Gaia* parallaxes. Then, we show the 3D map of the Milky Way's disk traced by classical Cepheids. In addition, we look into the future of periodic variable research in the era of *Gaia*, the Zwicky Transient Facility (Masci *et al.*, 2019; Graham *et al.*, 2019, ZTF), and the Large Synoptic Survey Telescope (LSST).

## 2 W UMa-type contact binaries

W UMa-type contact binaries are short-period variables ($P < 1$ day). Both components of the contact binary are close to each other and fill their Roche lobe. The materials are transferred between the two stars through a common envelope. The radius of the secondary star is limited

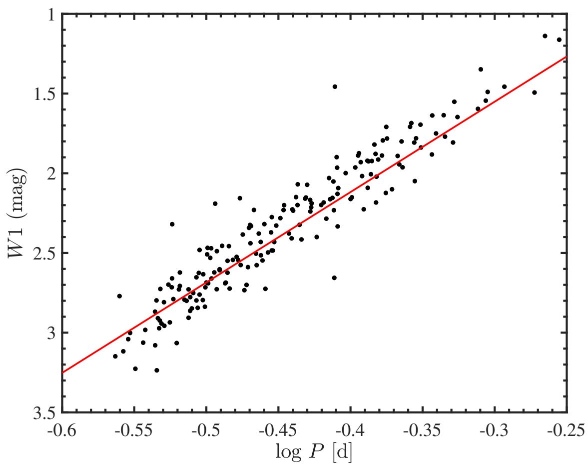


Figure 1: *WISE* $W1$ PLR for W UMa-type CBs using their maximum magnitudes. The black data points are the 183 W UMa-type CBs, while the red line is the best fit.

by the Roche limit, and as a result the total luminosity of the system is correlated to its orbital period. We selected 183 W UMa-type CBs within 330 pc. Based on *Gaia* DR2 parallaxes (Lindegren *et al.*, 2018; Luri *et al.*, 2018) and a Galactic extinction model, the absolute magnitudes of these CBs were estimated via $M_\lambda = m_\lambda - A_\lambda - (5\log 1/\varpi - 5)$. $M_\lambda$,$m_\lambda$, and $A_\lambda$ are the absolute magnitude, the apparent magnitude, and the extinction in a specific band, respectively. $\varpi$ here is the *Gaia* parallax in units of mas. Then, the PLRs were determined in 12 bands from the optical to the mid-infrared (Chen *et al.*, 2018a). Similarly to the classical Cepheids, the scatter ($1\sigma$ dispersion) of the CB PLRs decreases from the optical to the infrared bands. Hence, CB distances can be estimated more accurately in infrared bands. The equation for the maximum $W1$-magnitude PLR is $M_{W1}(\max) = -5.67\log P - 0.15, \sigma = 0.13$ mag (see Fig. 1). Here, the $W1$ band PLR shows a scatter of 0.13 mag (6% accuracy in distance).

The ages of the W UMa-type CB are in the range of 0.1–10 Gyr and show a peak at 4 Gyr. This intermediate-age tracer can fill the age gap between the young Cepheids and the old RR Lyrae. The number ratio of W UMa-type CBs is around 0.1–0.2% in the field, and as a result, the number of W UMa-type CB is significantly larger than that of other periodic variables. Based on the characteristic CB age and its large sample size, it is a crucial distance tracer for studying the detailed structure of our Milky Way.

## 3 Classical Cepheids

Classical Cepheids are the most important distance indicators on galaxy scales. However, the known Cepheids in our Milky Way are limited by the heavy extinction in the Galactic plane. Before 2018, only around 1000 Cepheids were known in our Galaxy. Based on new infrared and deep optical surveys, the number of classical Cepheids increased to 2330 (in 2018). Contaminants, such as type-II Cepheids and long period eclipsing binaries, were excluded with the help of *Gaia* DR2 parallaxes. We estimate the distances to these classical Cepheids using the multi-band optimal distance method with a combination of near-infrared and mid-infrared PLRs (Chen *et al.*, 2017; Wang *et al.*, 2018). After some selection choices, a 3D map of the Milky Way's disk was constructed based on 1339 Cepheids (see Fig. 2). The Cepheid sample covers about two-thirds of the disk from the Galactic center region to the outer disk (a distance of 20 kpc). The Milky Way's disk is clearly warped and flared. We adopted a warp model of $z_\mathrm{w} = a(R - R_\mathrm{w})^b \sin(\phi - \phi_\mathrm{w})$ to fit the distribution of the Cepheids. Here, $z_\mathrm{w}$, $a$, $R_\mathrm{w}$ and $\phi_\mathrm{w}$ are the warp height, its amplitude, its onset radius and the line of nodes (LON), respectively. The warp and flare of the Cepheid disk agree well with the gas disk in terms of their amplitudes. However, the LONs are different. The mean LON of the Cepheid warp deviates from the Galactic Center–Sun direction by $18^\circ$. Based on further analysis of the LON in each Galactocentric radius bin, we found that the LON is not stable but exhibits precession. In the radius range of 12–15 kpc, the LON increase as the radius increases. This leading pattern of the LON can be induced by torques from the inner disk and external material; torques owing to the massive inner disk are more dominant than those exerted by external material (Shen & Sellwood, 2006). In the kinematic map, the LON is also twisted and agrees with the spatial warp. This twisted LON is seen in the kinematic map of the upper main-sequence and giant stars (Poggio *et al.*, 2018).

At the same time, some questions have come up. One problem is whether the morphology of the warp varies when traced by stars of different ages (Amôres *et al.*, 2017; Wang *et al.*, 2019). This issue can be answered with the help of different distance indicators, such as contact binaries, Miras and red clump stars. Stars with better information on parallaxes and radial velocities included in future *Gaia* data releases will be useful to solve this problem. Another question relates to the morphology of the warp beyond 15 kpc. Is the warp lopsided (Romero-Gómez *et al.*, 2018) or even more complicated? This morphology can be investigated with a more completed sample of the Milky Way Cepheids based on *Gaia*, ZTF, and LSST.

## 4 Prospects of periodic variables

In *Gaia* DR 3, multi-epoch photometry will be available, and a catalog of periodic variables will be published. In addition, ZTF data release 1 became available in May 2019, and this catalog contains multi-epoch data obtained during the first nine months of the survey. Over the three-year ZTF survey, about 2 billion objects will have more than 100 single-exposure photometric data. By 2022, the number of periodic variables will have increased dramatically. The numbers of classical Cepheids, RR Lyrae, and contact binaries predicted to be found are listed in Table 1. The LSST is 6 times larger than the ZTF in diameter, and more than tens of millions of periodic variables will be found by the LSST.

Some periodic variables can be used to determine distances with both smaller statistical and smaller systematic errors. Based on an enlarged sample of periodic variables, we will uncover a more intuitive 3D map of the whole Milky Way. In addition, we will know the role of our Milky Way in the Local Group. Periodic variables can also be used to constrain the cosmological distance scale.

## Acknowledgments

We are grateful for research support from the Na-

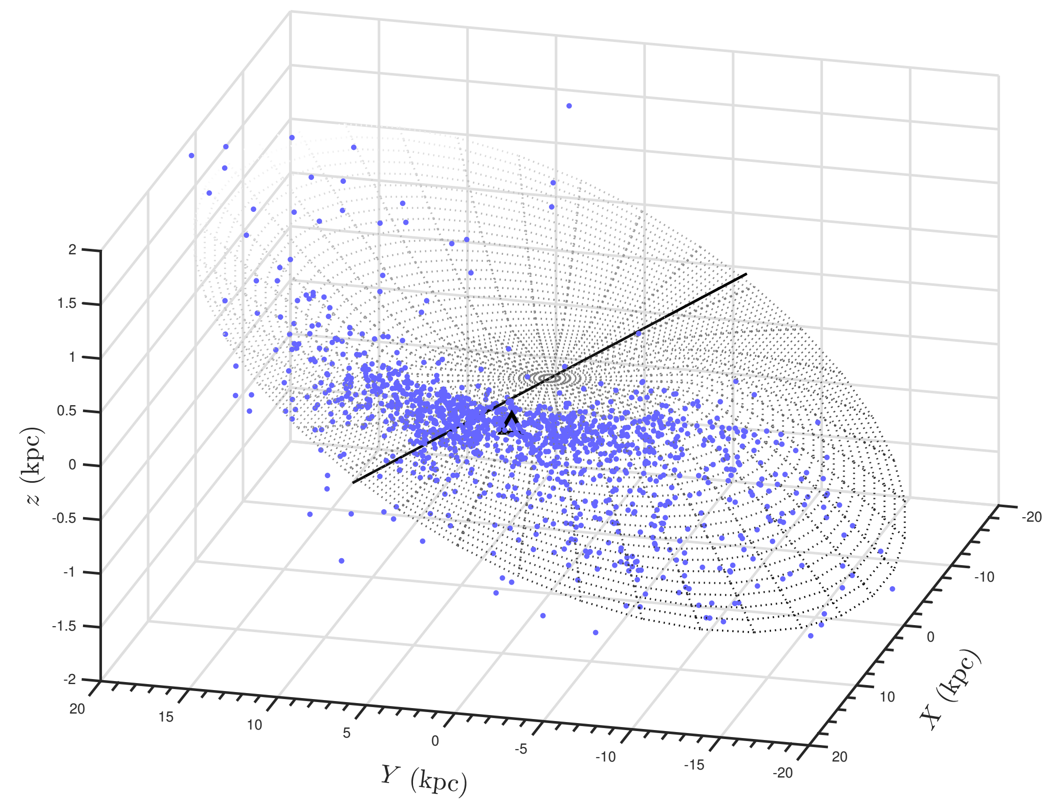


Figure 2: 3D map of the Milky Way's disk traced by 1339 classical Cepheids. The grid shows the best-fitting model of the warp. The black upward-pointing triangle is the position of the Sun. The solid black line is the mean line of nodes, which deviates from the Galactic Center–Sun direction by 18°.

Table 1: Information about periodic variables

| | Cepheids | RR Lyrae | Contact binaries |
|---|---|---|---|
| Distance accuracy | 3–5% | 3–5% | 6% |
| Age | 1–100 Myr | >10 Gyr | 100 Myr–10 Gyr |
| Number in Milky Way (Now) | 2000–3000 | ∼100,000 | ∼200,000 |
| Number in Milky Way (2022) | 6000–9000 | ∼200,000 | 1–2 million |

tional Natural Science Foundation of China through grants U1631102 and 11633005; from the Initiative Postdocs Support Program (No. BX201600002). This work was also supported by the National Key Research and Development Program of China through grant 2017YFA0402702. This work has made use of data from the European Space Agency (ESA) mission Gaia (https://www.cosmos.esa.int/gaia), processed by the Gaia Data Processing and Analysis Consortium (DPAC, https://www.cosmos.esa.int/web/gaia/dpac/consortium). Funding for the DPAC has been provided by national institutions, in particular the institutions participating in the Gaia Multilateral Agreement. This publication also makes use of data products from ALLWISE and NEOWISE, which are projects of the Jet Propulsion Laboratory/California Institute of Technology. ALLWISE and NEOWISE are funded by the National Aeronautics and Space Administration.

## References

Amôres, E. B., Robin, A. C., & Reylé, C. 2017, A&A, 602, A67.

Antoja, T., Helmi, A., Romero-Gómez, M., Katz, D., Babusiaux, C., *et al.* 2018, Nature, 561, 360.

Bhardwaj, A., Rejkuba, M., Minniti, D., Surot, F., Valenti, E., *et al.* 2017, A&A, 605, A100.

Chen, X., de Grijs, R., & Deng, L. 2016, ApJ, 832, 138.

Chen, X., de Grijs, R., & Deng, L. 2017, MNRAS, 464, 1119.

Chen, X., Deng, L., de Grijs, R., Wang, S., & Feng, Y. 2018a, ApJ, 859, 140.

Chen, X., Wang, S., Deng, L., de Grijs, R., Liu, C., *et al.* 2019, Nature Astronomy, 3, 320.
Chen, X., Wang, S., Deng, L., de Grijs, R., & Yang, M. 2018b, ApJS, 237, 28.
Clementini, G., Ripepi, V., Molinaro, R., Garofalo, A., Muraveva, T., *et al.* 2019, A&A, 622, A60.
Drake, A. J., Djorgovski, S. G., Catelan, M., Graham, M. J., Mahabal, A. A., *et al.* 2017, MNRAS, 469, 3688.
Drake, A. J., Graham, M. J., Djorgovski, S. G., Catelan, M., Mahabal, A. A., *et al.* 2014, ApJS, 213, 9.
Gaia Collaboration, Brown, A. G. A., Vallenari, A., Prusti, T., de Bruijne, J. H. J., *et al.* 2018, A&A, 616, A1.
Graham, M. J., Kulkarni, S. R., Bellm, E. C., Adams, S. M., Barbarino, C., *et al.* 2019, PASP, 131, 078001.
Heinze, A. N., Tonry, J. L., Denneau, L., Flewelling, H., Stalder, B., *et al.* 2018, AJ, 156, 241.
Jayasinghe, T., Kochanek, C. S., Stanek, K. Z., Shappee, B. J., Holoien, T. W. S., *et al.* 2018, MNRAS, 477, 3145.
Lindegren, L., Hernández, J., Bombrun, A., Klioner, S., Bastian, U., *et al.* 2018, A&A, 616, A2.
Luri, X., Brown, A. G. A., Sarro, L. M., Arenou, F., Bailer-Jones, C. A. L., *et al.* 2018, A&A, 616, A9.
Masci, F. J., Laher, R. R., Rusholme, B., Shupe, D. L., Groom, S., *et al.* 2019, PASP, 131, 018003.
Matsunaga, N., Bono, G., Chen, X., de Grijs, R., Inno, L., *et al.* 2018, SSRv, 214, 74.
Mowlavi, N., Lecoeur-Taïbi, I., Lebzelter, T., Rimoldini, L., Lorenz, D., *et al.* 2018, A&A, 618, A58.
Poggio, E., Drimmel, R., Lattanzi, M. G., Smart, R. L., Spagna, A., *et al.* 2018, MNRAS, 481, L21.
Romero-Gómez, M., Mateu, C., Aguilar, L., Figueras, F., & Castro-Ginard, A. 2018, arXiv e-prints, arXiv:1812.07576.
Shen, J. & Sellwood, J. A. 2006, MNRAS, 370, 2.
Wang, H. F., Huang, Y., Carlin, J. L., López-Corredoira, M., Chen, B. Q., *et al.* 2019, arXiv e-prints, arXiv:1905.11944.
Wang, S., Chen, X., de Grijs, R., & Deng, L. 2018, ApJ, 852, 78.